

A numerical simulation of dispersion and deposition of radioactive materials from the Fukushima Daiichi Nuclear Power Plant accident

MINGYUAN DU, SEIICHELIO YONEMURA

Institute for Agro-Environmental Sciences,
National Agriculture and Food Research Organization
3-1-3 Kannondai, Tsukuba, Ibaraki 305-8604
JAPAN

TOMOKI USHIYAMA

Public Works Research Institute
1-6 Minamihara, Tsukuba, Ibaraki, 305-8516
JAPAN

dumy@affrc.go.jp <https://researchmap.jp/read0082151/?lang=english>

Abstract: - Atmospheric numerical simulation models play a very important role for understanding dispersion and deposition processes of radioactive materials. Dispersion and deposition process of radioactive materials emitted from the Fukushima Daiichi nuclear power plant after the nuclear accident accompanied the great Tohoku earthquake and tsunami on 11 March 2011 were simulated using a pair of numerical models: A2Cflow and A2Ct&d. The model reproduced clearly the observed spatial distributions of deposition amount in main part of East Japan. Although there were some discrepancies between the simulated amount and observed amount somewhere, the simulation can explain when and why the special distributions were formed. These discrepancies were likely due to uncertainties in the simulation of emission rate due to no detail information of the emission rate.

Key-Words: - Cs-137, deposition amount; dispersion process; numerical simulation; radioactive material.

1 Introduction

A huge amount of radioactive materials was emitted into atmosphere from the Fukushima Daiichi nuclear power plant (FDNPP) after the nuclear accident accompanied the 9.0 magnitude Tohoku earthquake and tsunami on 11 March 2011 [1, 2]. These radioactive materials were dispersed or transported to East Japan, North America, Europe and cover much of the Northern Hemisphere and then deposited to the ground surface as shown both by actual measurements [e.g. 3, 4, 5, 6] and by numerical simulation [e.g. 7, 8, 9, 10, 11, 12, 13] soon after the accident. The short and long-range transport and deposition of the radioactive materials from FDNPP has been simulated by several numerical models soon after the accident [e.g. 7, 8, 9, 10, 11, 12, 13] and several years later [e.g. 14, 15]. In 2012 and in 2018, there were two special issues: Fukushima review and Fukushima review II on *Geochemical Journal* [16, 17], showing a number of researcher's works on the observations and simulations of deposition of the radioactive materials. However, notwithstanding more realistic simulations, progress is still to be made to accurately estimate people exposure due to the

release phase of the FDNPP accident [18]. In this study, we attempt to simulate this long-range atmospheric dispersion and deposition within East Japan (most of the Tohoku region and the Kanto region) with a pair of numerical models, A2Cflow and A2Ct&d by Yamada Science & Art [19, 20] to get a simulated accumulated deposition distribution map for explaining when and how the measured accumulated deposition distribution were formed for estimating people exposure at that time.

2 Model description

We used YSA's (Yamada Science and Art) A2C atmospheric modeling system (NEW HOTMAC/RAPTAD model) to simulate the local circulation and radioactive material dispersion with local circulations. A2C offers a high degree of accuracy in simulating, forecasting, and visualizing airflow and gas and particle dispersion in an urban environment—around buildings or over complex terrain. Superior quality 2-D and 3-D graphics along with a user-friendly interface make A2C an indispensable tool.

HORMAT is a three-dimensional numerical model for weather forecasting. The governing equations for mean wind, temperature, mixing ratio of water vapor, and turbulence are similar to those used by Yamada and Bunker [19]. Turbulence equation was based on the level 2.5 Mellor-Yamada [21, 22]. Five primitive equations were solved for ensemble averaged variables: three wind components, potential temperature and mixing ratio of water vapor. In addition, two primitive equations were solved for turbulence: one for turbulence kinetic energy and the other for a turbulence length scale [23]. The basic equations of HOTMAC were described in detail by Yamada and Bunker [21]. RAPTAD is a Lagrangian model in which a number of puffs are released at source and in which the change with time of puff characteristics, such as the location of the center and the size and age of the puff, is computed at every time step by using the air flow results deduced by MOTMAC. The basic equations of RAPTAD were described in detail by Yamada and Bunker [17] and some new features were discussed by Yamada [24] and Ushiyama et al. [20]. In this study, we added a deposition processes both dry and wet that will be described later.

2.1 Model domain and initial and meteorological condition

Three levels of model domain shown in Figure 1 were set with a 30 layers vertical structure with a surface layer thickness of about 10m and top layer to 5000m as follows:

Outer domain: 512km × 656km within 34°N-40°N and 137°E-143°E covered most of the Tohoku region and the Kanto region at an 8km grid resolution. Middle domain: 72km × 88km within 37°01'N-37°49'N and 140°18'E-141°08'E covered most of Fukushima prefecture at a 2km grid resolution. Inner domain: 10km × 10km within 37°22'N-37°27'N and 140°57'E-141°04'E covered the Fukushima Daiichi nuclear power plant (37°25'N, 141°02'E, FDNPP) at a 0.5km grid resolution.

Topographical data of Global 30' by U.S Geological Survey and the Japanese land use data for producing roughness, albedo, soil moisture, soil anthropogenic heat, soil conduction, soil specific heat, soil density and wetness were used in the simulation. The Japanese land use data is 100 m in resolution and the USGS data is 30 sec (approximately 800 m at mid latitudes) in resolution.

The three-dimensional meteorological fields from the Japan Meteorological Agency, GPV (Meso-Scale Model) data sets with about 10km × 10km

horizontal resolution for 3h intervals were used for initial and nudging analysis.

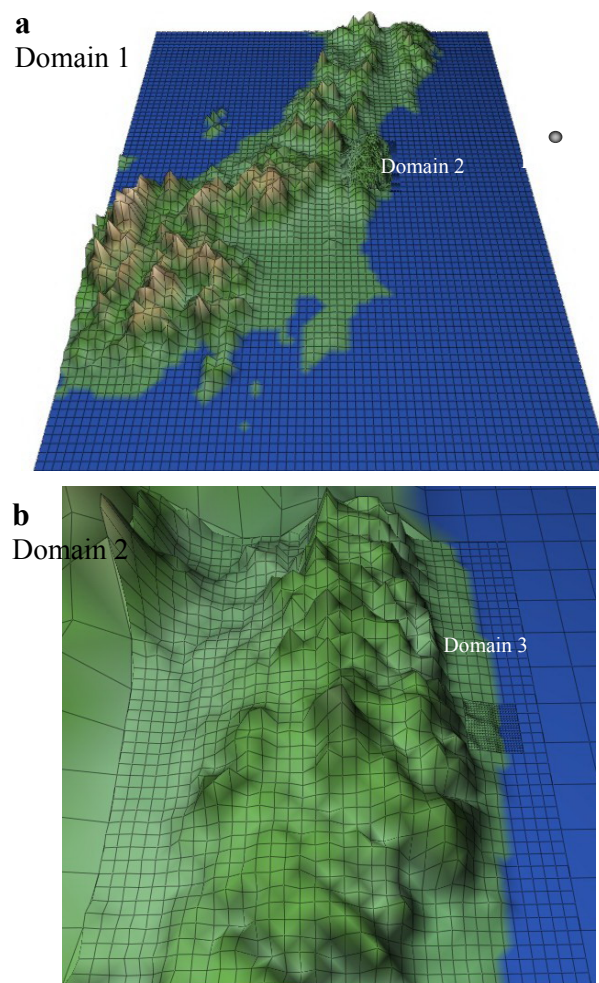


Fig. 1 Topography and simulation domain and grids size. a) Domain 1 and 2, b) Domain 2 and 3.

2.2 Emission

In the Raptad model the source material is represented by large numbers of model puffs released into the model atmosphere from any number of sources. Each puff of air represents a proportion of the mass or activity of a number of source species. In fact, an accurate assessment of the emission rates of the released radioactive materials would greatly enhance the accuracy of the deposition simulation. However, due to the uncontrolled nature of the release and the fact that the actual emission rate was not able to provide due to detailed information was not available for the study. Therefore, two possible emission scenarios, Chino et al.'s emission [8] and peak emission were used in our present simulations as shown in Figure 2.

Chino et al.'s data have a variable interval of 6–61 h (31 h on average), and we assumed that emission

rates were constant in each interval and only the rate for Cs-137 in Chino et al.'s data were used because we only considered Cs-137 and Cs-134 due to our objective was to get an accumulated deposition distribution for a long period. The radio-active decay was not considered.

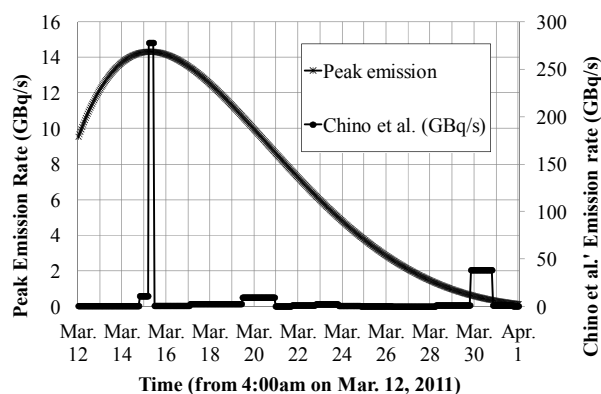


Fig. 2 Temporal variation of emission rate of 134C and 137C used in the model.

Peak emission was assumed that emission was a continued process such as began at 4 am on March 12 and reached its peak at 10am on March 15, 2011 and then decreased gradually with a function

$$Er = a(1 - (1 - t/L)^b)(k - t/L)^{b-1} \quad (1)$$

$(a > 0, b > 0 \text{ and } 0 < k \leq 1)$

where Er is the emission rate (Bq/s) at a given time t (s), a , b and k are coefficients of the used function and L is the period length from 4 am on March 12 in which released radioactive materials can be detected. In this simulation we assumed $a=168$, $b=3.75$, $L=600$ hours for having the total emission amount 12.6PBq as same as Chino et al.'s emission [8]. Therefore, our simulation was done for the period from 4 pm on March 12 to 0 am on April 1, 2011 (476hours).

2.3 Deposition

Dry deposition velocity of Cesium used in the simulation was 5.0×10^{-4} m/s.

For most pollutants wet deposition is the dominant means by which material is removed from the atmosphere to the ground. Two main processes are involved: washout, where material is 'swept out' by falling precipitation; and rainout, where material is absorbed directly into cloud droplets as they form by acting as cloud condensation nuclei. However, A2C Model does not simulate precipitation due to the precipitation microphysics are not tested well. We used Radar AMeDAS (Automated Meteorological Data Acquisition System) rain amount data as a input data for wet deposition. Radar AMeDAS data was 1km in resolution. Thus,

Rainout process was introduced only for the first rain encounter to dispersion of materials as following:

$$\text{Rainout} = \lambda C \quad (2)$$

where λ is first rain coefficient. In this simulation we assumed as 0.1.

The removal of material from the atmosphere by washout processes is considered below 1000m above the ground surface and based on the depletion equation

$$\frac{dC}{dt} = -\lambda C \quad (3)$$

where C is the concentration of radioactive materials, t is time, and λ the scavenging coefficient defined:

$$\lambda = \alpha r^\beta \quad (4)$$

where r is the rainfall rate and α and β are coefficients defined for different types of precipitation (e.g. rain and snow) as following [23]:

- rain: $\alpha = 8.4 \times 10^{-5}$, $\beta = 0.79$.
- snow: $\alpha = 8.0 \times 10^{-5}$, $\beta = 0.305$.

3 Results and discussions

3.1 Accumulated deposition and validation

Figure 3 shows the simulated spatial distributions of accumulated deposition (dry + wet) with a comparison with the observed results [3]. The deposition on the sea was ignored (deleted). The distribution pattern is very similar, especially for high concentration area No. ① and relative higher area No.④. Simulated relative higher areas No.② and No. ③ are bias to south. However, there are no relative higher concentration areas No. ⑤ and No. ⑥ and there is more distribution to the north of FDNPP. These discrepancies were likely due to uncertainties in the emission rate, treatment of deposition processes in the model, especially the uncertainty of emission rate. Simulation result in Figure 1 is the result of peak type emission. Chino's emission rate [8] induced a more discrepancy result due to his high emission rate in daytime on March 12 which would not be transported to Kanto Plain and high emission rate on March 30 which would reduce large deposition in whole East Japan. Yumimoto et al. [26] conducted an inverse analysis to optimally estimate the emission rate using the

time series of the deposition map, but the result is very different from that of [8] and [27].

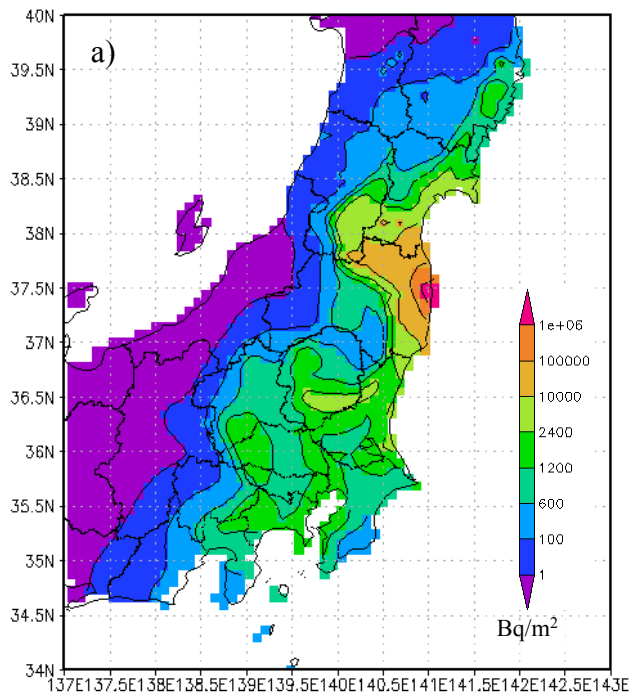


Fig. 3 a) Simulated (a) and observed [3] (b) spatial distributions of accumulated deposition of ^{134}Cs and ^{137}Cs . Numbers show the special distribution areas for comparison.

Fig. 3 b) Observed [3] spatial distributions of accumulated deposition of ^{134}Cs and ^{137}Cs . Numbers show the special distribution areas for comparison.

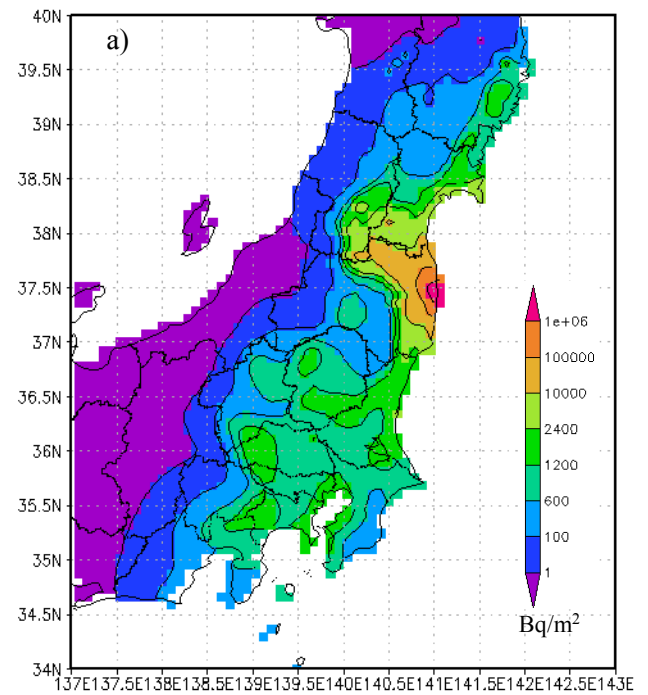


Fig. 4 a) Simulated spatial distributions of accumulated dry deposition of ^{134}Cs and ^{137}Cs .

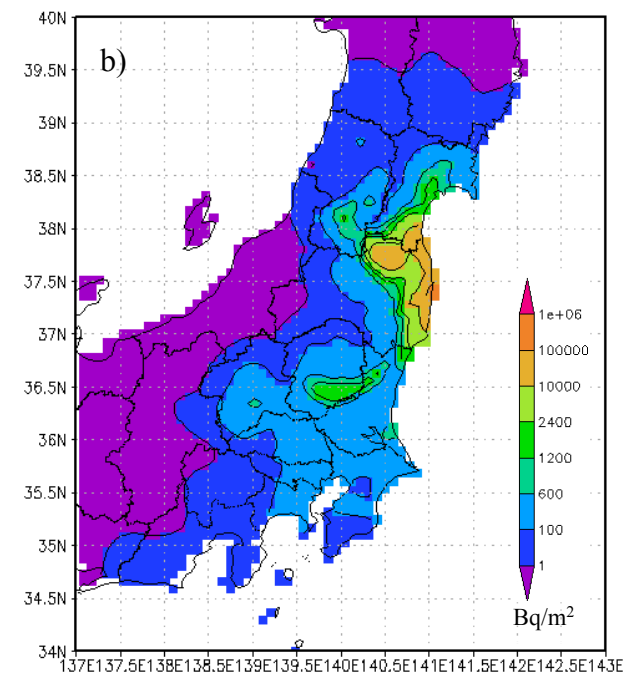
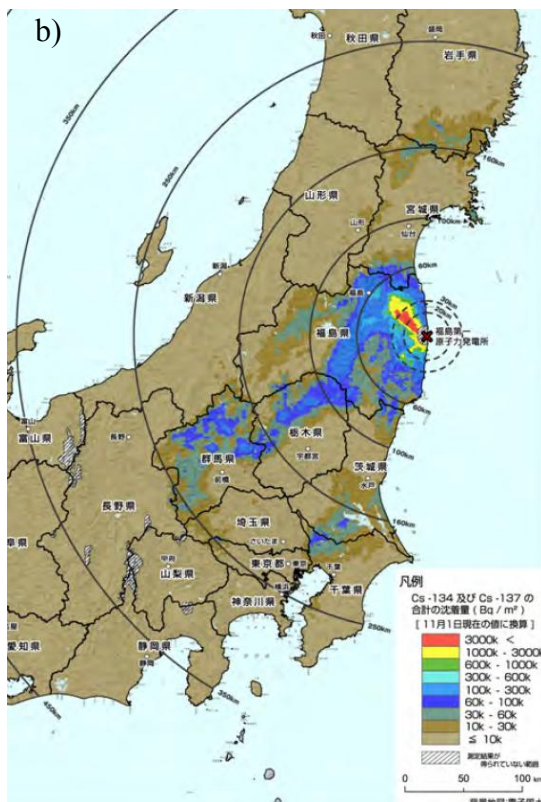


Fig. 4 b) Simulated spatial distributions of accumulated wet deposition of ^{134}Cs and ^{137}Cs .

As shown in Figure 4, the spatial pattern of accumulated deposition distribution was mainly formed by dry deposition, especially near the FDNPP and wet deposition has made the special distribution more complex far from the FDNPP. The ratio of wet and dry deposition in most area was about 0.5 to 1, but very large in the relative high concentration areas No. ③ to No. ⑤.

3.2 Dispersion processes

Figure 5 shows a simple time series of the dispersion processes of the radioactive materials as following:

- 1) Although emission was started at about 4am, Mar. 12, first dispersion to the land (area No.

①) was started at 13pm, Mar. 12 (Julian day 71) (Fig. 5 a)) and ended at about 19pm on Mar. 12 (Fig. 5 b)). This dispersion was due to combination of local land (at night) and sea (during day time) breeze and mountain (during day time) and valley (at night) wind. This type of dispersion was happened 11 times during the simulated 20 days such as shown in Fig.5 e) and h). Dispersion process was that the radioactive materials emitted from FDNPP dispersed directly to northeast (So called Iitatemura, area No. ①) in the afternoon and then back to east during night time.

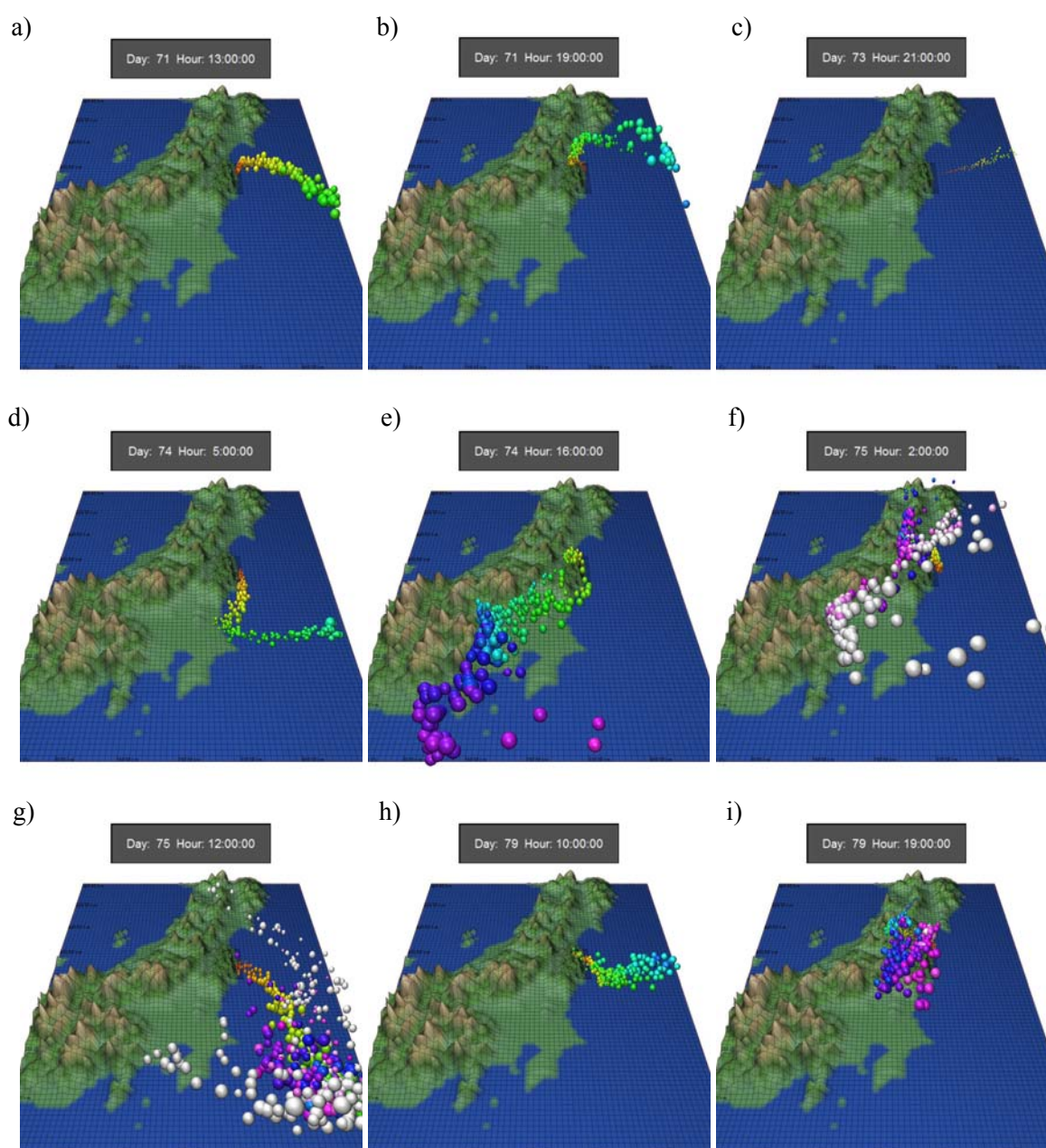


Fig. 5 a) – i) Temporal variation of three-dimensional special distribution of model puffs released into the model atmosphere showing the dispersion processes of radioactive materials. (day is Julian day of the year)

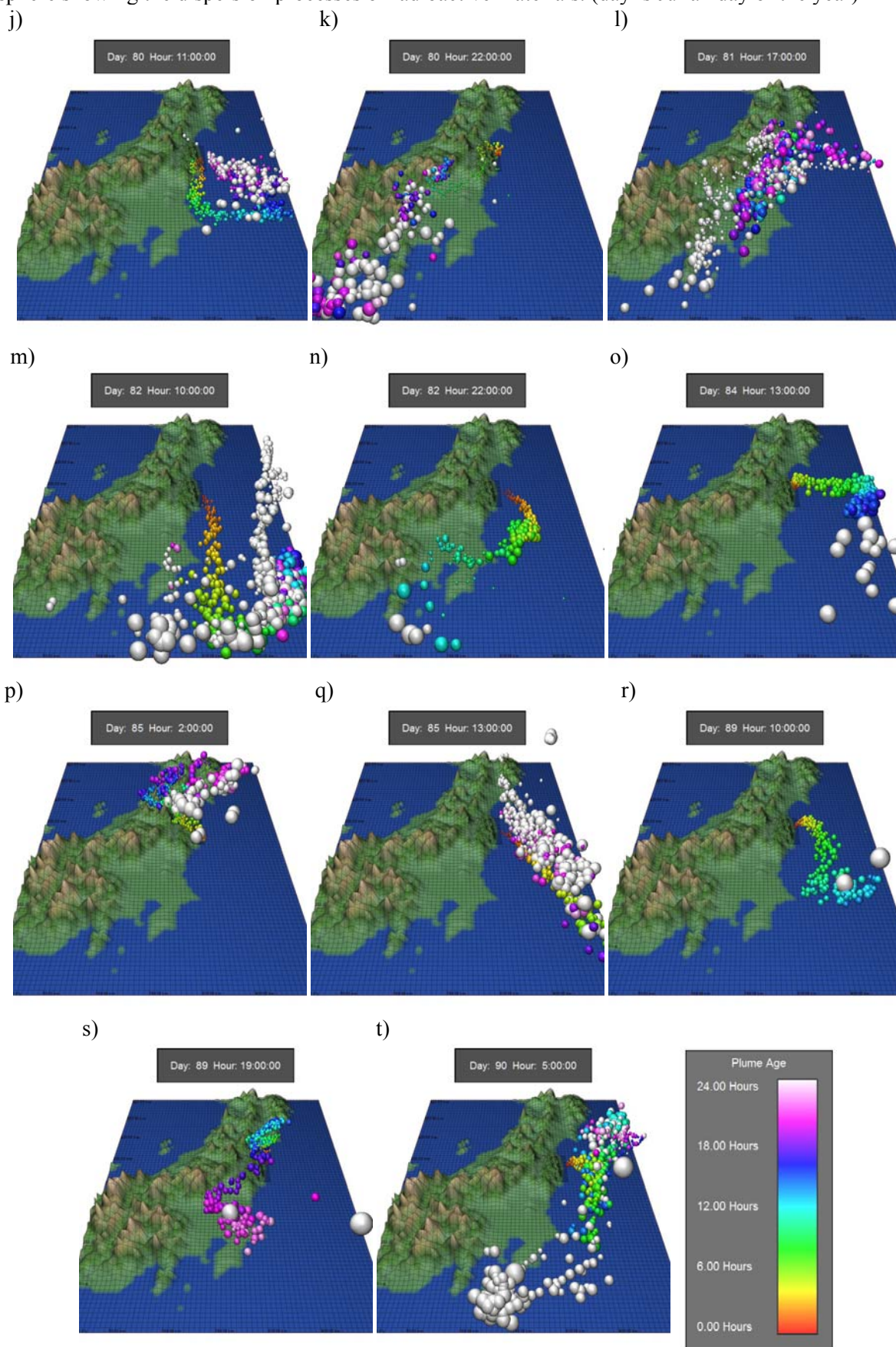


Fig. 5 j) – t) Temporal variation of three-dimensional special distribution of model puffs released into the model atmosphere showing the dispersion processes of radioactive materials. (day is Julian day of the year)

- 2) Basic dispersion was eastward during most of simulation time period as shown in Fig.5 c) and h) due to the prevailing west wind in March. Extensive dispersions to whole East Japan were only occurred 3 times: Mar. 15 to 16 (Fig. 5 d) to g)), Mar. 21 to 23 (Fig. 5 j) to m)) and Mar. 30 (Fig. 5 r) to t)) due to low-pressure system traveling across Japan. This process was as following: The radioactive materials emitted from FDNPP was firstly transported eastward as shown in Fig.5 c) and h) and then transported to south over the sea as shown in Fig. 5 d) and j). These large amount radioactive materials were transported westward to East Japan as shown in Fig. 5 e) and k) and then northward (Fig. 5 f) and l)) and then back to southeast (Fig. 5 g) and m)). These were responsible for the extensive deposition to East Japan.
- 3) There were two times of dispersion only to the Tohoku region but not to the Kanto region: Mar.20 and Mar. 25 (Fig. 5 h) and i)) to 26 (Fig. 5 o) to q) due to low-pressure system passing over.
- 4) There was only one case that land and sea breeze in Kanto region bring the radioactive materials from sea to land as shown in Fig. 5 n).

3.3 Deposition processes

The processes of accumulated deposition distribution shown in Fig. 3 can be divided to 3 steps due to the dispersion processes as mentioned above. Figure 6 shows the 3 steps as following:

Step 1, 13pm to 19pm JST on Mar. 12: Higher concentration distribution area (so called Iitate mura) to the northwest of the FDNPP was formed soon after the emission during the first land and sea breeze from 13pm to 19pm JST on Mar. 12 as shown in Fig.6 a). Only dry deposition occurred during this step shown in Fig.6 b).

Step 2, 4pm on Mar.15 to 12pm on Mar 16: Basic distribution pattern was formed during the first low-pressure system traveling across Japan from 4pm on Mar.15 to 12pm on Mar 16 as shown in Fig. 6 c). This pattern was mainly formed by dry deposition as shown in Fig. 6 d). Only small amount of wet deposition occurred in the Kanto region and some wet deposition occurred to the northwest of FDNPP as shown in Fig.6 e).

Step 3, Mar. 21 to 23: Final distribution pattern and amount was formed mostly after the low-pressure system traveling across Japan during Mar. 21 to 23

as shown in Fig.6 f). Both dry and wet deposition was occurred. Wet deposition was the main process and more important for the formation of the distribution as shown in Fig. 6 g) and h).

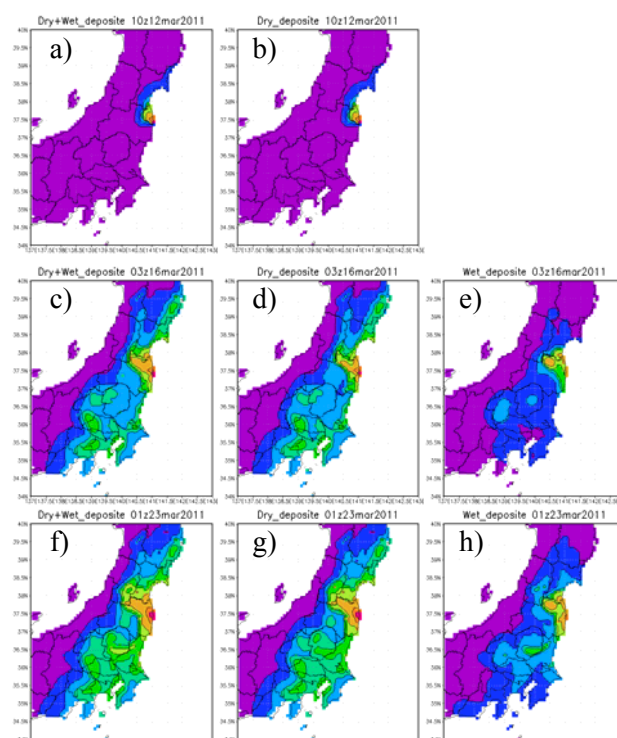


Fig. 6 Temporal variation of simulated spatial distribution of dry, wet and total (dry+wet deposition) showing the deposition processes of radioactive materials. (Time is GMT)

4 Conclusion

Dispersion and deposition process of radioactive materials were simulated using a pair of numerical models, A2Cflow and A2Ct&d. The model reproduced clearly the observed spatial distributions of deposition amount in main part of East Japan. Although there were some discrepancies between the simulated amount and observed amount somewhere, we can conclude that the basic accumulated deposition pattern was mainly formed by dry deposition and wet deposition has made the special distribution more complex. The dispersion and deposition processes can be summarized as three steps. First step during the afternoon on Mar. 12 formed higher concentration area to the northwest of FDNPP by dry deposition. Second step from Mar. 15 to Mar. 16 forms the basic distribution pattern mainly by dry deposition. Third step determined the

final distribution both by dry and wet deposition and wet deposition played more important roles.

Detailed emission rate information and wet deposition process would improve the numerical simulation results.

This paper is a revised version of a paper entitled “Numerical simulation of dispersion and deposition of radioactive materials from the Fukushima Daiichi nuclear power plant in March of 2011” presented at the 2nd International Conference on Integrated Systems and Management for Energy, Development, Environment and Health (ISMAEDELH '13) Morioka City, Iwate, Japan, April 23-25, 2013.

Acknowledgements

The authors thank Dr. Tetsuji Yamada (Yamada Science and Art) for his valuable advice and suggestions throughout the analysis. We also thank Dr. Masaru Chiba (Academic express, Inc.) for his intensive support on the programming and suggestions for the simulation. The GFD Dennou Club Library and Grid Analysis and Display System (GrADS) were used to draw the figures. The GPV analysis data were produced by the Japan Meteorological Agency and reformatted into NetCDF by the Research Institute for Sustainable Humanosphere, Kyoto University.

References:

- [1] Nuclear Safety Commission of Japan. Trial estimation of emission of radioactive materials (I-131, Cs-137) into the atmosphere from Fukushima Dai-ichi Nuclear Power Station, Tokyo, 2011, <http://www.nsc.go.jp/NSCenglish/geje/2011%200412%20press.pdf>.
- [2] Butler, D. Radioactivity spreads in Japan, *Nature*, 471(7340), 2011, pp. 555-556.
- [3] MEXT (Ministry of Education, Culture, Sports, Science and Technology). Monitoring information of environmental radioactivity level. 2011, <http://radioactivity.mext.go.jp/en/>.
- [4] Momoshima, N., S. Sugihara, R. Ichikawa, H. Yokoyama, Atmospheric radionuclides transported to Fukuoka, Japan remote from the Fukushima Daiichi nuclear power complex following the nuclear accident, *Journal of Environmental Radioactivity*, 111, 2012, pp. 28-32.
- [5] Bowyer, T.W., S.R. Biegalski, M. Cooper, P.W. Eslinger, D. Haas, J.C. Hayes, H.S. Miley, D.J. Strom, V. Woods, Elevated radioxenon detected remotely following the Fukushima nuclear accident, *Journal of Environmental Radioactivity*, 102, 2011, pp. 681-687.
- [6] Bolsunovsky, A. and D. Dementyev, Evidence of the radioactive fallout in the center of Asia (Russia) following the Fukushima Nuclear Accident. *Journal of Environmental Radioactivity*, 102, 2011, pp. 1062-1064.
- [7] Takemura T., H. Nakamura, M. Takigawa, H. Kondo, T. Satomura, T. Miyasaka and T. Nakajima, A Numerical Simulation of Global Transport of Atmospheric Particles Emitted from the Fukushima Daiichi Nuclear Power Plant, *SOLA*, 7, 2011, pp. 101-104.
- [8] Chino, M., H. Nakayama, H. Nagai, H. Terada, G. Katata, and H. Yamazawa, Preliminary Estimation of Release Amounts of ¹³¹I and ¹³⁷Cs Accidentally Discharged from the Fukushima Daiichi Nuclear Power Plant into the Atmosphere, *Journal of Nuclear Science and Technology*, 48, 2011, pp. 1129-1134.
- [9] Morino, Y. T. Ohara, and M. Nishizawa, Atmospheric behavior, deposition, and budget of radioactive materials from the Fukushima Daiichi nuclear power plant in March 2011, *Geophysical Research Letters*, 38, 2011, pp. doi:10.1029/2011GL049689.
- [10] Qiao F., G. Wang, W. Zhao, J. Zhao, D. Dai, Y. Song and Z. Song, Predicting the spread of nuclear radiation from the damaged Fukushima Nuclear Power Plant, *Chinese Science Bulletin*, 56, 2011, pp. 1890-1896.
- [11] Leelossy, A., Mészáros, R., Lagzi, I., Short and long term dispersion patterns of radionuclides in the atmosphere around the Fukushima Nuclear Power Plant. *Journal of Environmental Radioactivity*, 102, 2011, pp. 1117-1121.
- [12] Katata, G., H. Terada, H. Nagai, M. Chino, Numerical reconstruction of high dose rate zones due to the Fukushima Daiichi Nuclear Power Plant accident, *Journal of Environmental Radioactivity*, 111, pp. 2-12.
- [13] Yasunari TJ, Stohl A, Hayano RS, Burkhart JF, Eckhardt S, Yasunari T., Cesium-137 deposition and contamination of Japanese soils due to the Fukushima nuclear accident. *PNAS* 108, 2011, pp. 19530-19534. doi:10.1073/pnas.1112058108.
- [14] Yumimoto, K., Y. Morino, T. Ohara, Y. Oura, M. Ebihara, H. Tsuruta and T. Nakajima. Inverse modeling of the ¹³⁷Cs source term of the Fukushima Dai-ichi Nuclear Power Plant accident constrained by a deposition map

- monitored by aircraft. *Journal of Environmental Radioactivity*, 164, 2016, pp. 1–12.
- [15] Nakajima, T.; Misawa, S.; Morino, Y.; Tsuruta, H.; Goto, D.; Uchida, J.; Takemura, T.; Ohara, T.; Oura, Y.; Ebihara, M.; et al. Model depiction of the atmospheric flows of radioactive cesium emitted from the Fukushima Daiichi Nuclear Power Station accident. *Prog. Earth Planet. Sci.* 2017, 4:2. DOI 10.1186/s40645-017-0117-x.
- [16] Ebihara, M., Yoshida, N. and Takahashi, Y., Preface: Migration of radionuclides from the Fukushima Daiichi Nuclear Power Plant accident. *Geochem. J.* 46, 2012, pp. 267–270.
- [17] Y Takahashi, H Qin, CM Yeager, Q Fan, Fukushima Review II on migration of radionuclides from the Fukushima Daiichi Nuclear Power Plant accident, *Geochem. J.* 52, 2018, pp. 81–83.
- [18] Mathieu, A., M. Kajino, I. Korsakissok, R. Périllat, D. Quélo, A. Quérel, O. Saunier, T. T. Sekiyama, Y. Igarashi, D. Didier, Fukushima Daiichi–derived radionuclides in the atmosphere, transport and deposition in Japan: A review. *Applied Geochemistry*, 91, 2018, pp. 122-139.
- [19] Yamada, T., and S. Bunker, Development of a nested grid, second moment turbulence closure model and application to the 1982 ASCOT Brush Creek data simulation, *J. Appl. Meteor.* 27, 1988, pp. 562-578.
- [20] Ushiyama, T., M. Du, S. Inoue, H. Shibaie, S. Yonemura, S. Kawashima, and K. Amano, Three-dimensional prediction of maize pollen dispersal and cross-pollination and their suppression by windbreaks, *Environmental Biosafety Research*, 8, 2009, pp. 183-202.
- [21] Mellor, G. L. and T. Yamada, A Hierarchy of Turbulence Closure Models for Planetary Boundary layers, *J. of Atmos. Sci.*, 31, 1974, pp. 1791-1806.
- [22] Mellor, G. L. and T. Yamada, Development of a Turbulence Closure Model for Geophysical Fluid Problems, *Rev. Geophys. Space Phys.*, 20, 1982, pp. 851-875.
- [23] Yamada, T, Simulations of Nocturnal Drainage Flows by a q2l Turbulence Closure Model, *J. of Atmos. Sci.*, 40, 1983, pp. 91-106.
- [24] Yamada, T, Numerical Simulations of Airflows and Tracer Transport in the Southern United States, *Journal of Applied Meteorology*, 39, 2000, pp. 399-411.
- [25] Nelson, N., K.P. Kitchen, R. Maryon, Assessment of routine atmospheric discharges from the Sellafield nuclear installation—Cumbria UK, *Atmospheric Environment*, 36, 2002, pp. 3203–3215.
- [26] Yumimoto K, Morino Y, Ohara T, Oura Y, Ebihara M, Tsuruta H, Nakajima T (2016) Inverse modeling of the ¹³⁷Cs source term of the Fukushima Dai-ichi Nuclear Power Plant accident constrained by a deposition map monitored by aircraft. *Journal of Environmental Radioactivity*, 164, 2016, pp. 1–12.
- [27] Katata G, Chino M, Kobayashi T, Terada H, Ota M, Nagai H, Kajino M, Draxler R, Hort MC, Malo A, Torii T, Sanada Y., Detailed source term estimation of the atmospheric release for the Fukushima Daiichi Nuclear Power Station accident by coupling simulations of an atmospheric dispersion model with an improved deposition scheme and oceanic dispersion model. *Atmos Chem Phys*, 15, 2015, pp.1029–1070.